Translational Oncology
www.transonc.com

Volume 3 Number 3 June 2010 pp. 153–159 153

In Vivo Bioluminescent Imaging of Irradiated Orthotopic Pancreatic Cancer Xenografts in Nonobese Diabetic–Severe Combined Immunodeficient Mice: A Novel Method for Targeting and Assaying Efficacy of Ionizing Radiation

Cheong J. Lee*, Aaron C. Spalding†, Edgar Ben-Josef†, Lidong Wang* and Diane M. Simeone*,‡

*Department of Surgery, University of Michigan, Ann Arbor, MI, USA; †Department of Radiation Oncology, University of Michigan, Ann Arbor, MI, USA; ‡Department of Molecular and Integrative Physiology, University of Michigan, Ann Arbor, MI, USA

Abstract

Adenocarcinoma of the pancreas is a lethal malignancy, and better models to study tumor behavior *in vivo* are needed for the development of more effective therapeutics. Ionizing radiation is a treatment modality that is commonly used in the clinical setting, in particular, for locally confined disease; however, good model systems to study the effect of ionizing radiation in orthotopic tumors have not been established. In an attempt to create clinically relevant models for studying treatments directed against pancreatic cancer, we have defined a methodology to measure the effect of varying doses of radiation in established human pancreatic cancer orthotopic xenografts using two different pancreatic cancer cell lines (Panc-1 and BXPC3) infected with a lentiviral vector expressing CMV promoter–driven luciferase to allow bioluminescence imaging of live animals in real time. Quantifiable photon emission from luciferase signaling *in vivo* correlated well with actual tumor growth. Bioluminescence imaging of the established pancreatic xenografts was used to direct delivery of radiation to the orthotopic tumors and minimize off-target adverse effects. Growth delay was observed with schedules in the range of 7.5 Gy in five fractions to 10 Gy in four fractions, whereas doses 3 Gy or higher produced toxic adverse effects. In conclusion, we describe a model in which the effects of ionizing radiation, alone or in combination with other therapeutics, in orthotopic xenografts, can be studied.

Translational Oncology (2010) 3, 153–159

Introduction

Adenocarcinoma of the pancreas ranks fourth highest in cancer-related mortality in the United States. In 2008, an estimated 34,000 people were diagnosed with pancreatic cancer that has an overall 5-year survival of less than 5% [1]. Although major advancements have been made in understanding the disease, effective therapeutic regimens are still lacking. There is a great need for relevant preclinical models to test potential therapeutics in the treatment of pancreatic cancer.

The use of animal models that mimic biological processes of cancer seen in human disease is paramount in testing potential therapeutics. Many researchers use human xenografts established in immune-deficient animals to recapitulate the biologic behavior of tumors. When implanted subcutaneously in an animal, tumor biometrics are easy to monitor. The establishment of tumors in the subcutis, however, may not necessarily represent the most appropriate niche to study cancers that arise in other sites because studies have shown the tumor microenvironment to be an integral component that influences the response of tumors to therapeutics [2–5]. In contrast, orthotopic transplantation of primary human tumors in immune-deficient mice reproduces a pattern of local growth and distal dissemination seen in humans. It has been shown that orthotopically implanted pancreatic tumors in

Address all correspondence to: Diane M. Simeone, MD, Surgery and Molecular and Integrative Physiology, TC 2210B, Box 5343, University of Michigan Medical Center, 1500 E Medical Center Dr, Ann Arbor, MI 48109. E-mail: simeone@umich.edu
Received 13 July 2009; Revised 17 December 2009; Accepted 29 December 2009

 1944-7124/10/$25.00
DOI 10.1593/tlo.09184

immune-deficient mice closely mimic human tumors in their growth and metastatic potential [6–8]. However, without *in vivo* imaging capability, orthotopic models require sacrifice of the animal to assess treatment effect and thus limit the real time evaluation of treatment effects in living animals.

In vivo imaging techniques of mouse models of human disease, namely magnetic resonance imaging or computed tomographic scans, can be costly and time-consuming. An alternative approach for *in vivo* imaging is abdominal ultrasound [9], which may be less costly, but high-throughput evaluation of therapeutics is limited by the requirement of highly skilled personnel to interpret the studies. The use of fluorescence and bioluminescence has proven utility in *in vivo* studies of the pancreas and other organ systems [10–12]. In this study, we investigate the effect of ionizing radiation on xenografts established orthotopically in nonobese diabetic–severe combined immunodeficient (NOD/SCID) mice and develop a method to deliver ionizing radiation treatment to orthotopically implanted pancreatic tumors based on biometrics gathered from luciferase-based bioluminescent imaging.

Materials and Methods

Cell Lines

Panc-1 and BXPC3 human pancreatic cancer cells were obtained from the American Type Culture Collection (Manassas, VA) and were maintained in Roswell Park Memorial Institute medium containing 10% bovine serum in an atmosphere of 93% air and 7% carbon dioxide. Both cell lines were transduced with nonreplication competent lenitvirus from the viral vector core of the University of Michigan expressing a CMV promoter 5′ to the firefly luciferase protein followed by green florescent protein tag. Pancreatic cancer cell lines were plated at 2×10^5 cells/well in six-well plates. The cells were allowed to adhere for 12 hours, after which the medium was replaced with 2 ml of either 1:500 or 1:5000 diluted viral concentrate. The number of cells per well was counted at the time of virus addition, and the average of four wells was used to calculate the viral titer. Viral supernatants remained on the cells for 48 hours, after which the cells are analyzed for expression of luciferase *in vitro* through FACS sorting for green florescent protein. Transfection efficiency was measured to be higher than 99% when transfection was performed with MOI = 5. Luciferase activity was assessed by detection of photons using the Xenogen IVIS system (Xenogen, Alameda, CA) after administration of 150 μg/ml D-luciferin to cells incubated 2 minutes after administration of substrate.

Subcutaneous and Orthotopic Xenografts

Animals used in this study were maintained in facilities approved by the American Association for Accreditation of Laboratory Animal Care in accordance with current regulations and standards of the US Department of Agriculture and Department of Health and Human Services. The animal protocol used in this study was approved by the University Committee on Use and Care of Animals at the University of Michigan. For subcutaneous implantation of tumor, 1×10^6 BXPC3 or Panc-1 cells were injected subcutaneously into the flanks of mice using a 26.5-gauge needle after deep anesthesia was induced. To establish orthotopic xenografts, after administration of anesthesia, a small subcostal laparotomy was performed, and BXPC3 or Panc-1 cells infected with the lentivirus-expressing luciferase (BXPC3-Luc or Panc-1–Luc, respectively) were then injected orthotopically in concentrations of 1×10^6 cells in the pancreatic tail of NOD/SCID mice.

Bioluminescent Imaging

For *in vivo* imaging, mice were given the substrate D-luciferin (150 mg/kg in PBS) by intraperitoneal injection immediately after administration of anesthesia with isoflurane (1%-3%). Two minutes after administration of substrate, the anesthetized mice were placed onto the warmed stage inside the light-tight camera box with continuous exposure to isoflurane (1%-2%). In this study, animals were imaged 2 minutes after luciferin injection to ensure consistent photon flux. In our study, measuring 2 minutes after luciferin injection gave a result within a range of 15% variability. The mice were imaged twice weekly for 21 to 28 days depending on experimental conditions or until tumor burden was too great, as defined by significant weight loss, development of abdominal ascites, or respiratory failure. The acquisition time data for photon emission measurement were normalized to 120 seconds. The IVIS camera system was used to visualize the tumors, and photon measurement was defined around the tumor area and quantified as total photon/s using Living Image software (Xenogen, Corp, Alameda, CA). Tumor size was determined after necropsy at varying time points, and correlation was made with average photon emission after live animal imaging.

Irradiation

Orthotopically implanted animals were randomized to radiation treatment or placebo once mean tumor volume reached approximately 200 mm^3. Animals were irradiated in the Radiation Core of the University of Michigan Comprehensive Cancer Center (Ann Arbor, MI) using a Phillips 250 Orthovoltage unit (Philips Medical Systems, Farmington Hills, MI) at approximately 1.4 Gy/min to the animals. Dosimetry was carried out using an ionization chamber connected to an electrometer system directly traceable to a National Institute of Standards and Technology calibration. Mice were anesthetized with a mixture of ketamine 60 mg/kg and xylazine 3 mg/kg, and positioning was guided by bioluminescent images of the tumor signal and was confirmed by clinical tumor palpation such that the tumor was at the center of a 2.4-cm aperture in the secondary collimator. Mice were focally irradiated after being appropriately shielded from radiation using size-appropriate lead aprons fashioned to expose only the area of tumor (adjustable lead shielding which allows exposure of area as small as 1.0 cm) while protecting the animals. A half-beam block technique was used to ensure a nondivergence of the radiation beam edge.

Statistical Analysis

Analysis of variance was used to determine the significance of differences of tumor photon emissions between various radiation schedules. Differences between treated and untreated groups in tumor volume were tested for significance with two-tailed Student's *t*-test. The xenograft studies were powered at 80% to detect a 30% difference in photon emissions.

Results

Quantifiable Photon Emission Detected by Luciferase Signaling In Vivo Is a Function of Mean Tumor Volume

Signal intensity from orthotopic tumors was measured by quantified photon emission of the luciferase activity of tumors at different time points after implantation. After measurement, animals were killed, and actual tumor volume was measured. Tumor volume measurements correlated well with mean quantified photon emission detected for both BXPC3 and Panc-1 orthotopic xenografts. A nonlinear regression

analysis was performed to estimate a growth curve based on photon emission. R^2 values for curve fit approached close to 1 for both xenografts: BXPC3, $R^2 = 0.837$, $P < .05$; and Panc-1, $R^2 = 0.905$, $P < .01$ (Figure 1). The measured luciferase activity between the two xenografts was different. Mean photon emission of BXPC3 tumors at 300 mm^3 in size was higher than Panc-1 tumors at 300 mm^3 in size ($3.284\ e^8 \pm 3.106\ e^8$ *vs* $1.289\ e^8 \pm 5.583\ e^7$ p/sec per square centimeters per steradian, $n = 5$, $P < .05$).

Comparison of Subcutaneous and Orthotopically Implanted Pancreatic Cancer Cells

Surgical implantation of luciferase expressing BXPC3 and Panc-1 (1×10^6) cells into the subcutis or orthotopically in the pancreatic tail was performed, and tumor biometrics were compared among the two tumor implant sites. None of the mice died of anesthetic or surgical complications. Tumor size and metastasis were assessed at necropsy 21 days after tumor cell implantation. There was gradual tumor enlargement of both orthotopic and subcutaneous tumors after implantation, which correlated with increased photon emission based on bioluminescent imaging. Tumor kinetics was not significantly different between the orthotopic and subcutaneous tumors for the first 21 days; however, the growth of the orthotopic tumors was found to plateau from day 21 (Figure 2*A*). Table 1 shows necropsy results of mice implanted with either orthotopic or subcutaneous tumors at 21 days. Approximately 90% (18/20 BXPC3, 17/20 Panc-1) of the orthotopic implantations succeeded in tumor formation, whereas all of the subcutaneous implantations formed tumors (8/8). Orthotopic tumor implants had, on average, smaller tumor volume in comparison to subcutaneous implants at 21 days (Figure 2*B*): BXPC3 tumors, 416 mm^3 orthotopic *versus* 1145 mm^3 subcutaneous; and Panc-1 tumors, 254 mm^3 orthotopic *versus* 756 mm^3 subcutaneous. There was a significantly higher incidence of metastasis with orthotopic implants in comparison to subcutaneous implants (23/35 [71%] of orthotopic implants *vs* 2/16 [12%] of subcutaneous implants). The predominant area of local invasion in the orthotopically implanted tumors was invasion of the stomach followed by invasion of the duodenum and spleen. The most common site of distant metastasis was the liver, followed by lung. Liver and lung metastasis could be detected by bioluminescence from day 10 (10 ± 4.5) and later (data not shown). However, quantification and characterization of the metastatic implants were performed by gross examination at necropsy, and bioluminescence was reserved for assessment of the treatment effect on the primary tumor because this was the focus of this study. Some tumors resulted in massive tumor growth resulting in life-threatening bowel obstruction. BXPC3 cells were more locally aggressive in comparison to Panc-1 cells, displaying increased tumor size when implanted orthotopically (416 *vs* 254 mm^3, $P < .05$); however, rates of metastasis were not statistically different (14/18 *vs* 11/17, P = NS).

Minimal Radiation Toxicity and Good Clinical Efficacy Is Observed with Fractionated Dosing Regimens of 1.5 to 2 Gy per Fraction

The effect of radiation on tumor growth was determined using a number of fractionated regimens, with the dose per fraction varying from 1.5 to 3 Gy. Tumor suppression was seen with all doses of fractionated radiation in both cell lines (Figure 3*A*). The degree of tumor suppression was proportional to the increase in radiation dose used. Significant toxicity was seen with radiation doses of 3 Gy. Non–tumor-bearing animals were irradiated, and weight loss was determined as a measure of toxicity. Significant weight loss occurred at a radiation dose of 3 Gy, with greater than 30% weight loss occurring 5 days after radiation (data not shown). With 1.5 to 2 Gy doses administered for 5 days, only a 5% to 10% reduction in weight occurred at day 5, and stable weights resumed (Figure 3*B*). With 2.5 Gy of radiation administered daily for 4 days, a mean of 25% weight loss occurred during ionizing radiation treatment but regained weight once treatment ceased

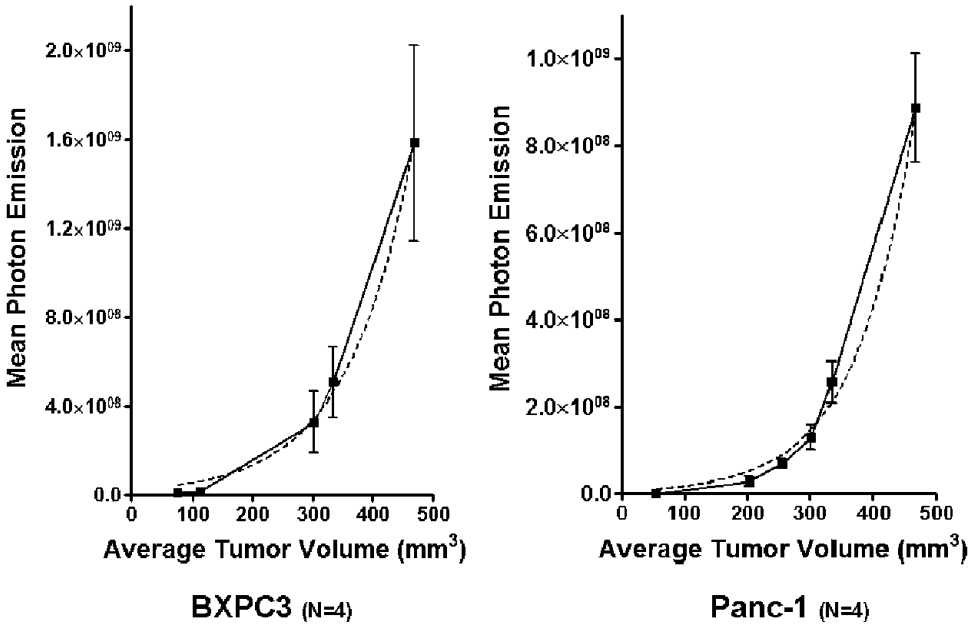

Figure 1. Quantifiable photon emission from luciferase signaling *in vivo* is a function of mean tumor volume. Regression analysis of mean photon emission as a function of tumor volume showed that R^2 values approached 1. For BXPC3 tumors, the R^2 curve fit was 0.837 ($P < .05$); for Panc-1 tumors, this was 0.905 ($P < .01$).

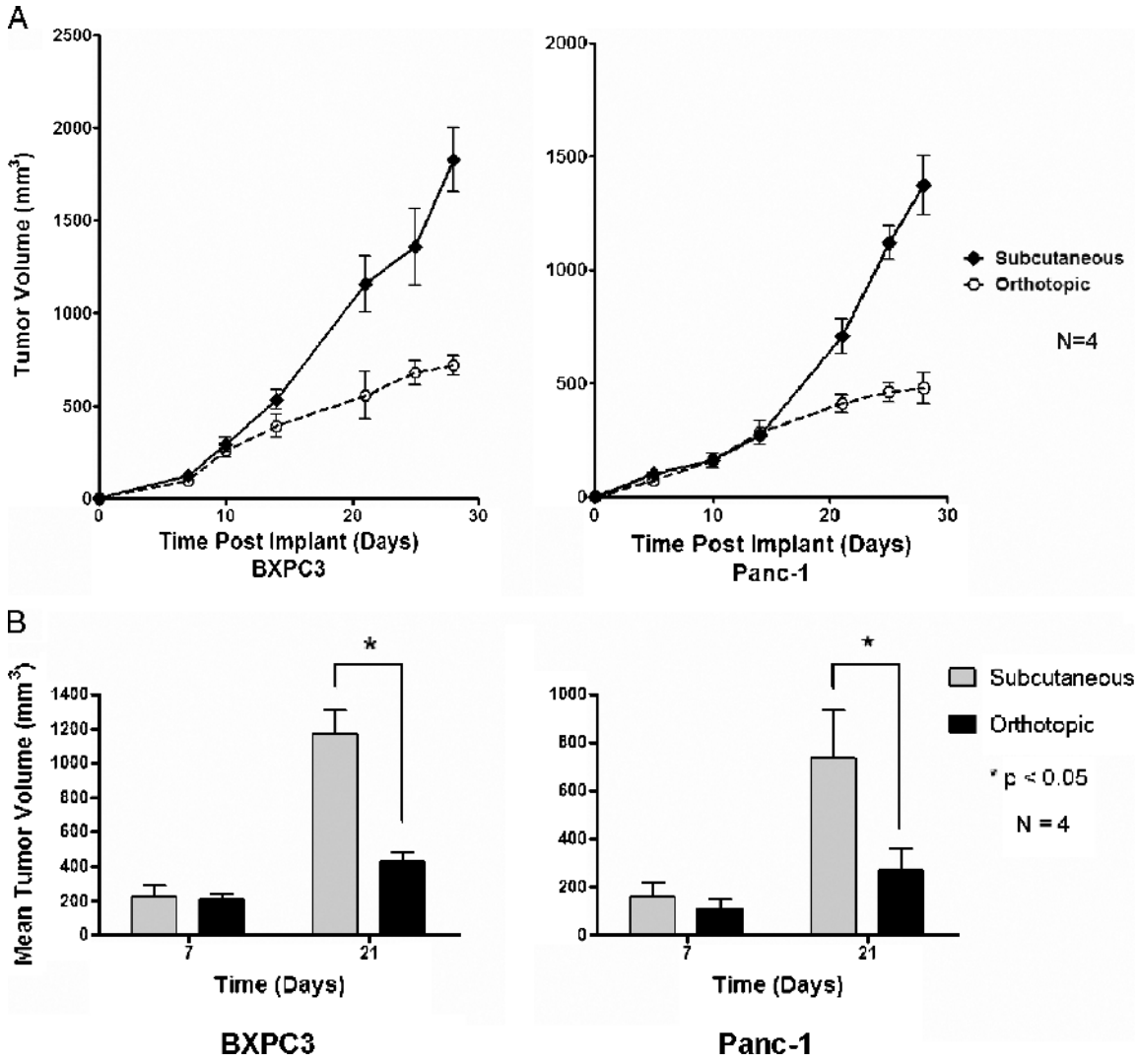

Figure 2. Comparison of subcutaneous and orthotopically implanted cancer cells. Comparison of tumor kinetics and growth between subcutaneous and orthotopic xenografts of BXPC3 (right) and Panc-1 (left) after implantation of 1×10^6 cells. (A) Each data point consists of tumor analysis from four animals. (B) Mean tumor volume of subcutaneous and orthotopic tumors at 7 and 21 days.

(Figure 3*B*). On the basis of these data, the range of dose of ionizing radiation that produced tumor growth delay without undue toxicity was between 1.5 Gy × 5 fractions (7.5 Gy total) and 2.5 Gy × 4 fractions (10 Gy total); doses beyond this level produced toxic adverse effects.

Quantifiable Photon Emission from In Vivo Luciferase Activity Correlated with Tumor Growth Suppression from Ionizing Radiation

The measured signal intensity of BXPC3 and Panc-1 xenografts showed significant reduction in luciferase activity after ionizing radiation treatment (Figure 4*A*). The mean quantified photon emission of BXPC3 tumors at 10 days after 2.5 Gy × 4 fractions was significantly less than control tumors: $3.781\ e^8 \pm 3.330e^8$ p/sec per square centimeters per steradian (untreated) *versus* $1.332\ e^8 \pm 8.359e^7$ p/sec per square centimeters per steradian (treated), $n = 4$, $P < .05$ (Figure 4*B*, *left panel*). A similar decrease in luciferase signal intensity was seen in Panc-1 xenografts at 10 days after radiation treatment of 2.5 Gy × 4; $2.429\ e^8 \pm 2.12\ e^8$ p/sec per square centimeters per steradian (untreated) *versus* $1.304\ e^8 \pm 5.917\ e^7$ p/sec per square centimeters per steradian (treated), $n = 4$, $P < .05$ (Figure 4*B*, *right panel*). A significant reduction in tumor

Table 1. Primary and Metastatic Growth of BXPC3 and Panc-1 Orthotopic and Subcutaneous Xenografts in NOD/SCID Mice.

	No. Implanted	Graft Take	Stomach Invasion	Duodenal Invasion	Spleen Invasion	Liver Met	Lung Met	Bowel Met	Peritoneum	No. Animals with Distant Met
Orthotopic implants										
BXPC3	20	18	18	15	8	8	7	6	11	14
Panc-1	20	17	16	15	5	6	4	3	9	11
Subcutaneous implants										
BXPC3	8	8	0	0	0	1	1	0	2	2
Panc-1	8	8	0	0	0	0	0	0	1	1

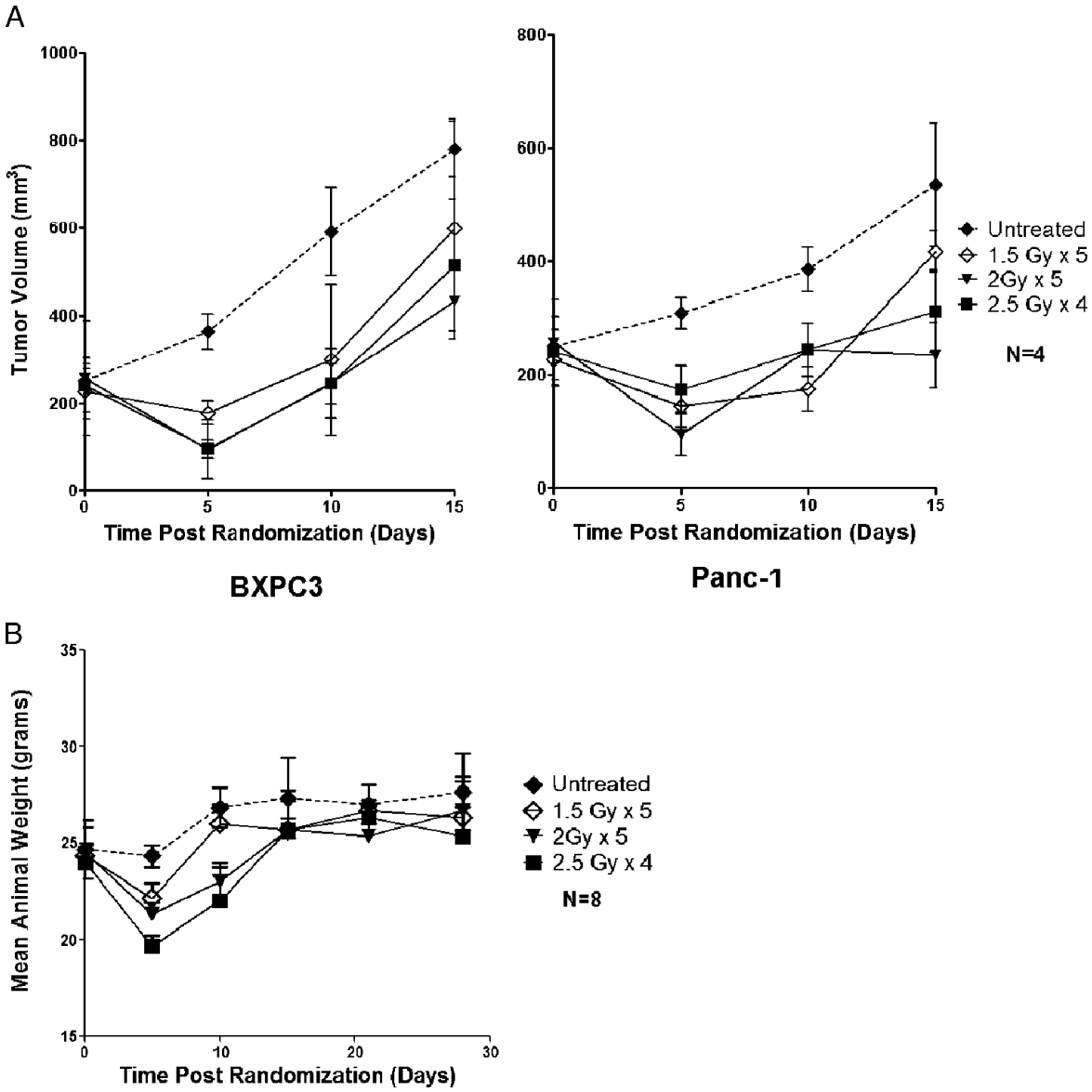

Figure 3. Minimal radiation toxicity is observed with fractionated dosing regiments of 2 to 2.5 Gy. Orthotopic xenograft response to irradiation. Animals were randomized to irradiation *versus* placebo once they reached a tumor volume of approximately 200 mm^3. (A) All tested radiation schedules reduced orthotopic tumor volume. Each data point is the analysis of data from four animals. (B) Animal weight changes were minimal (<10% decline) with 1.5- to 2.5-Gy fraction doses of radiation. Each data point consists of tumor analysis of eight animals.

volume was seen at the 10-day period of BXPC3 tumors: 441 ± 105.1 mm^3 (untreated) *versus* 163 ± 90.73 mm^3 (treated), $n = 4$, $P < .05$ (Figure 4*C*, *left panel*). The effect of radiation on Panc-1 xenografts was also significant, where mean tumor volume was greater in the untreated group (286.7 ± 105.9 mm^3) compared with the treated group (111.0 ± 40.9 mm^3; $n = 4$, $P < .05$; Figure 4*C*, *right panel*). After the cessation of treatment, tumor suppression abated, and tumor recovery and growth were observed in BXPC3 xenografts 21 days after radiation treatments were stopped. In the Panc-1 xenografts, tumor volume at 28 days after radiation treatment showed continued tumor suppression. In contrast, in the BXPC3 tumors, there was a small tumor mass reduction that did not reach statistical significance (Figure 4*C*, *left panel*). The mean tumor volume of BXPC3 xenografts at 28 days after radiation treatment was 667.7 ± 120.6 *versus* 768.4 ± 133.3 mm^3 in nonirradiated controls, $n = 4$, P = NS. Mean tumor volume of Panc-1 tumors at 28 days after randomization was measured to be 574.0 ± 79.5 mm^3 in the untreated arm of the experiment *versus* 253 ± 77.1 mm^3 in the treated animals ($n = 4$, $P < .05$).

Discussion

In this report, we demonstrate the successful use of bioluminescence imaging to direct radiation delivery to orthotopic pancreatic cancer xenografts, an animal model of pancreatic cancer that faithfully recapitulates some of the most important features of the human malignancy, such as local invasion and metastasis. We also show that bioluminescence allows monitoring of tumor biometrics by both visualization of spread and quantification of tumor size in real time in the same animal as they undergo treatment.

The use of luciferase activity to measure tumor biometrics after antitumor therapy has been described previously [13]. However, there are only few reports on the use of radiation to treat orthotopic xenografts, and they are mostly found in prostate and brain tumor research

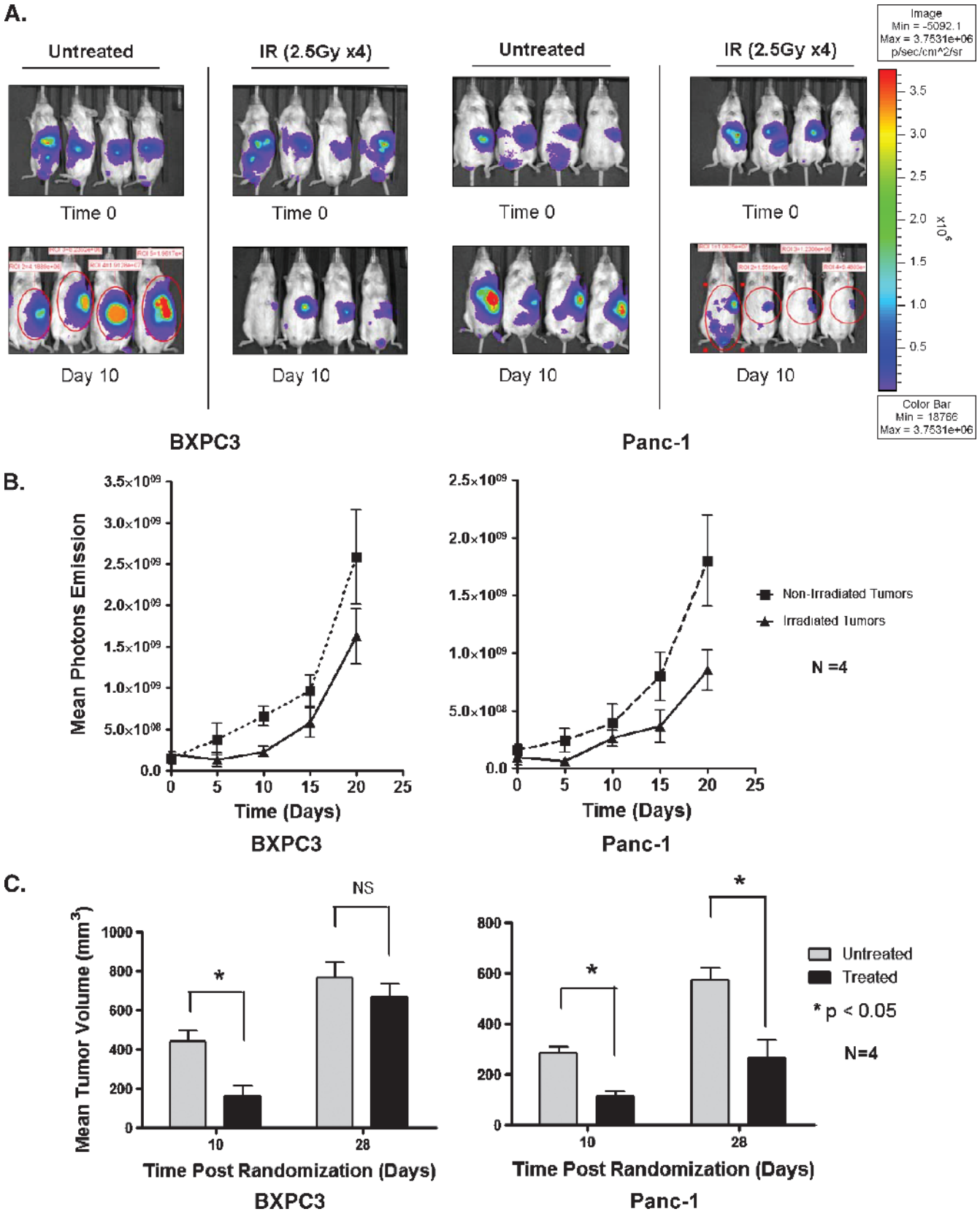

Figure 4. Quantifiable photon emission from *in vivo* luciferase signaling correlated with tumor suppression from ionizing radiation. Mice implanted orthotopically with BXPC3-Luc or Panc-1–Luc were treated with placebo or four fractions of 2.5 Gy. Same four mice from each treatment group are shown in consistent pairings throughout the experiment. (A) Some figures may illustrate means of data acquisition (red ovals) used to quantify photon emission. (B) Both tumor lines experienced growth delay after irradiation, as measured by photon emission. (C) Collection of the tumors at day 10 after radiation therapy revealed detectable differences in tumor size in both xenografts. However, at day 28 after cessation of radiation, only Panc-1 tumors continued to show tumor suppression.

[14–16]. Previous work in brain tumors has entailed the use of one [14] or two [15] fractions in nude mice and has focused on the study of short-term effects, without attempting to maintain the animals alive for prolonged periods. Freytag et al. [16] did use SCID mice, but they, too, delivered only two fractions. Our work is unique in the application of *in vivo* bioluminescence image guidance to direct radiation focally at a target surrounded by sensitive abdominal organs in an extraordinarily radiosensitive animal. Using this method, we described a range of multifraction dose schedules (that better approximate clinical radiotherapy regimens), which allow a quantitative assessment of the antitumor effect of radiation, during a protracted period.

In our study, we did find differential luciferase activity between the two tumor cell lines BXPC3 and Panc-1. As both tumor lines were analyzed to have equivalent transfection efficiencies, differential expression of luciferase does not explain the findings we see in this study. To put it simply, it is possible that there are less tumor cells in Panc-1 tumors; this may result in less emission. When tumors were further analyzed histologically, a more potent peritumoral desmoplasia was seen in Panc-1 tumors. We believe that enhanced stromal proliferation may contribute to the discrepancy seen in luciferase activity between Panc-1 and BXPC3 tumors. Stromal proliferation leading to desmoplasia may play a significant role in inhibition of the luciferin penetrance and delivery to tumor cells or result in a relative inhibition of photon emission within these tumors. Alternatively, the density of cancer cells within the more desmoplastic tumor microenvironment may be less, resulting in a weaker luciferase signal.

In summary, the data we present demonstrate that luciferase imaging of orthotopically established pancreatic xenografts accurately assesses tumor growth *in vivo*. Importantly, orthotopic radiation of NOD/SCID mice is feasible without compromising overall mouse survival allowing for longitudinal studies of tumor treatment effect and outcome. This novel system for studying *in vivo* tumor growth and suppression provides a clinically relevant model for assessing the efficacy of various therapeutics used in combination with radiation. As such, it represents an important tool in the development of new, more effective, regimens to be used in unresectable tumors as well as in the adjuvant or neoadjuvant setting. In addition, this system may also be a useful investigative model to locate and harvest residual tumors in treated animals to study mechanisms underlying resistance to therapy.

References

[1] Jemal A, Siegel R, Ward E, Hao Y, Xu J, Murray T, and Thun MJ (2008). Cancer statistics, 2008. *CA Cancer J Clin* **58**, 71–96.

[2] Fidler IJ (1995). Modulation of the organ microenvironment for treatment of cancer metastasis. *J Natl Cancer Inst* **87**, 1588–1592.

[3] Dumont N and Arteaga CL (2002). The tumor microenvironment: a potential arbitrator of the tumor suppressive and promoting actions of TGFβ. *Differentiation* **70**, 574–582.

[4] Dalton WS (1999). The tumor microenvironment as a determinant of drug response and resistance. *Drug Resist Updat* **2**, 285–288.

[5] Jung YD, Ahmad SA, Akagi Y, Takahashi Y, Liu W, Reinmuth N, Shaheen RM, Fan F, and Ellis LM (2000). Role of the tumor microenvironment in mediating response to anti-angiogenic therapy. *Cancer Metastasis Rev* **19**, 147–157.

[6] Mohammad RM, Al-Katib A, Pettit GR, Vaitkevicius VK, Joshi U, Adsay V, Majumdar AP, and Sarkar FH (1998). An orthotopic model of human pancreatic cancer in severe combined immunodeficient mice: potential application for preclinical studies. *Clin Cancer Res* **4**, 887–894.

[7] Capellá G, Farré L, Villanueva A, Reyes G, García C, Tarafa G, and Lluís F (1999). Orthotopic models of human pancreatic cancer. *Ann N Y Acad Sci* **880**, 103–109.

[8] Schwarz RE, McCarty TM, Peralta EA, Diamond DJ, and Ellenhorn JD (1999). An orthotopic *in vivo* model of human pancreatic cancer. *Surgery* **126**, 562–567.

[9] Ziske C, Tiemann K, Schmidt T, Nagaraj S, Märten A, Schmitz V, Clarenbach R, Sauerbruch T, and Schmidt-Wolf IG (2008). Real-time high-resolution compound imaging allows percutaneous initiation and surveillance in an orthotopic murine pancreatic cancer model. *Pancreas* **36**, 146–152.

[10] Bouvet M, Wang J, Nardin SR, Nassirpour R, Yang M, Baranov E, Jiang P, Moossa AR, and Hoffman RM (2002). Real-time optical imaging of primary tumor growth and multiple metastatic events in a pancreatic cancer orthotopic model. *Cancer Res* **62**, 1534–1540.

[11] Caceres G, Zhu XY, Jiao JA, Zankina R, Aller A, and Andreotti P (2003). Imaging of luciferase and GFP-transfected human tumours in nude mice. *Luminescence* **18**, 218–223.

[12] Olivo C, Albias J, Verweij V, Van Zonneveld AJ, Dhert WJ, and Martens AC (2008). *In vivo* bioluminescence imaging study to monitor ectopic bone formation by luciferase gene marked mesenchymal stem cells. *J Orthop Res* **26**, 901–909.

[13] El Hilali N, Rubio N, Martinez-Villacampa M, and Blanco J (2002). Combined noninvasive imaging and luminometric quantification of luciferase-labeled human prostate tumors and metastases. *Lab Invest* **82**, 1563–1571.

[14] Camphausen K, Purow B, Sproull M, Scott T, Ozawa T, Deen DF, and Tofilon PJ (2005). Orthotopic growth of human glioma cells quantitatively and qualitatively influences radiation-induced changes in gene expression. *Cancer Res* **65**, 10389–10393.

[15] Sarkaria JN, Carlson BL, Schroeder MA, Grogan P, Brown PD, Giannini C, Ballman KV, Kitange GJ, Guha A, Pandita A, et al. (2006). Use of an orthotopic xenograft model for assessing the effect of epidermal growth factor receptor amplification on glioblastoma radiation response. *Clin Cancer Res* **12**, 2264–2271.

[16] Freytag SO, Paielli D, Wing M, Rogulski K, Brown S, Kolozsvary A, Seely J, Barton K, Dragovic A, and Kim JH (2002). Efficacy and toxicity of replication-competent adenovirus-mediated double suicide gene therapy in combination with radiation therapy in an orthotopic mouse prostate cancer model. *Int J Radiat Oncol Biol Phys* **54**, 873–885.